Articles

Restricted Swelling and Its Orientation Effect on Copolymer Micellar Solutions of Hexagonal-Packed Cylinders under Steady Shear Flow

J. Grandjean† and A. Mourchid*,‡

IFP-Lyon, BP 3, 69390 Vernaison, France, and Matière et Systèmes Complexes, UMR 7057 Centre National de la Recherche Scientifique-Université Paris VII, 75205 Paris cedex 13, France

Received June 22, 2007. In Final Form: December 13, 2007

We investigate the structure of polystyrene-*b*-poly(acrylic acid, sodium salt) copolymer in aqueous solutions. We offer detailed characterization of the micellar solutions by scattering techniques and show that they form hexagonal-packed cylinders. The micelles follow the swelling law expected for cylinders, upon addition of water, down to a concentration threshold below which the distance cylinder−cylinder remains constant. The results suggest that the cylinders are aggregated. It is proposed that this micellar association is the cause of the unusual orientation of the cylinders in a steady shear flow field, where the cylinder axis is found to be parallel to the velocity gradient.

Introduction

The need for engineered soft materials is increasing considerably as a consequence of the demand for novel combinations of properties by the emerging technologies.[1] In this respect, block copolymers have proven to be very suitable and versatile materials in nanoscience and nanotechnology.[1,2] They have the ability to self-assemble at the mesoscopic length scale (tens of nanometers) either in melt, in solution of selective solvents, or in blends with a homopolymer that interacts specifically with one constitutive block.[3−5] Self-assembly yields the formation of a variety of ordered phases. Amphiphilic diblock copolymers exhibit characteristic equilibrium morphologies as a result of the balance between the enthalpic penalty originating from contacts between the two dissimilar blocks and the entropic constraint imposed by the covalent linkage between them.[3] These morphologies are spherical, rodlike, or lamellar micelles, and their formation is governed by both the length of each block and the interblock repulsion strength.[6] In blends and in solution, the composition of the blocks and their interaction with the dispersing phase further force the phase morphology.[7,8] Comprehensive theoretical and experimental studies were reported on the nanostructural organization of block copolymers, and the effects of other relevant parameters, such as volume fraction and temperature, were carefully studied. Consequently, it is now easy to fully control the phase morphology by adjusting these parameters.[9]

Stacked lamellae and hexagonal-packed cylinders (HPC) are two common phases of block copolymer anisometric micelles and are classified as liquid crystalline phases.[10] These ordered phases are induced by long-range orientation correlations between the micelles.[11] They are characterized by a director orientation in addition to the positional order. However, the samples are usually not aligned to the macroscopic length scale level, and polydomain structures are present which yield textures recognizable from polarizing optical microscopy studies.[10] The textures are a feature of the mesophase structure and do not depend on the molecular detail, since the restricted alignment of a broad variety of anisotropic species yields similar textures.

When block copolymers are subjected to shear, structural changes are commonly induced.[12,13] Similar structure changes occur in a large number of systems such as liquid crystalline solutions of stiff molecules, thermotropic liquid crystals, microemulsions, and colloidal suspensions as well as in block copolymer melts and solutions.[14] In particular, structures under shear of aqueous solutions of amphiphilic block copolymers that form anisotropic morphologies are of special interest.[15] Their liquid crystal structure can be strongly disrupted by the application of a flow field. Often, complex flow properties are observed even though in most cases these anisotropic species tend to align with the longest axis parallel to the shear direction, v. This arrangement minimizes drag resistance and yields two typical orientational configurations for lamellae, with their normal either parallel to the velocity gradient direction, ∇v, or to the neutral or vorticity direction, z.[16,17] These two configurations are referred to as parallel or perpendicular orientations. In particular, it was

† IFP-Lyon.

‡ UMR 7057 Centre National de la Recherche Scientifique-Université Paris VII.

(1) Park, C.; Yoon, J.; Thomas, E. L. *Polymer* **2003**, *44*, 6725−6760.
(2) Hamley, I. W. *Nanotechnology* **2003**, *14*, R39−R54.
(3) Hamley, I. W. *The Physics of Block Copolymers*; Oxford University Press: New York, 1998.
(4) Riess, G. *Prog. Polym. Sci.* **2003**, *28*, 1107−1170.
(5) Akiyama, M.; Jamieson, A. M. *Polymer* **1992**, *33*, 3582−3592.
(6) Jackson, C. L.; Barnes, K. A.; Morrison, F. A.; Mays, J. W.; Nakatani, A. I.; Han. C. C. *Macromolecules* **1995**, *28*, 713−722.
(7) Lipic, P. M.; Bates, F. S.; Matsen, M. W. *J. Polym. Sci., Part B: Polym. Phys.* **1999**, *37*, 2229−2238.
(8) Matsen, M. W.; Bates, F. S. *Macromolecules* **1996**, *29*, 1091−1098.
(9) Jiang, R.; Jin, Q.; Li, B.; Ding, D. *Macromolecules* **2006**, *39*, 5891−5896.
(10) Wang, W.; Hashimoto, T. *Polymer* **2000**, *41* 4729−4735.
(11) Forster, S.; Berton, B.; Hentze, H.-P.; Krämer, E.; Antonietti, M.; Lindner, P. *Macromolecules* **2001**, *34*, 4610−4623.
(12) Hamley, I. W. *J. Phys.: Condens. Matter* **2001**, *13*, R643−R671.
(13) Koppi, K. A.; Tirrell, M.; Bates, F. S. *J. Rheol.* **1994**, *38*, 999−1027.
(14) Larson, R. G. *The Structure and Rheology of Complex Fluids*; Oxford University Press: New York, 1999.
(15) Hamley, I. W. *Curr. Opin. Colloid Polym. Sci.* **2000**, *5*, 342−350.
(16) Koppi, K. A.; Tirrell, M.; BaColl.tes, F. S.; Almdal, K.; Colby, R. H. *J. Phys. II* **1992**, *2*, 1941−1959.
(17) Pople, J. A.; Hamley, I. W.; Fairclough, J. P. A.; Ryan, A. J.; Hill, G.; Price, C. *Polymer* **1999**, *40*, 5709−5714.

10.1021/la703764e CCC: $40.75
Published on Web 02/07/2008

shown that these two configurations represent a common behavior of lamellae of diblock copolymers subjected to large amplitude oscillations or steady shear flow. For these copolymers, the effect of chain entanglement is negligible and so are the resulting topological constraints. For lamellar morphologies of high molecular weight diblock copolymers, it was shown that entanglement between neighboring lamellae affects the alignment and promotes the transverse configuration where the normal to the lamellae is found toward the velocity direction.[18] A similar orientation was also observed in a concentrated temperature-induced lamellar phase of a low molecular weight diblock polymer at low shear rate[17] and was later hypothesized to be a nonequilibrium state probably due to sample loading.[12]

The condition of minimal drag resistance confines the block copolymer cylinders, subjected to a flow field, in the shear plane (shear and vorticity plane) pointing toward the shear axis.[19] Furthermore, for HPC, the densely packed layers of cylinders, the planes (10) of the hexagonal unit cell, are often found to be parallel to the shear plane.[20] This configuration is known as parallel orientation as against perpendicular orientation where the cylinders still point toward the shear direction with the densely packed layers of cylinders perpendicular to the shear plane. It was shown that this last configuration is favored when the sheared HPC phase is close to the order−disorder transition temperature.[21] All alternative configurations, where the cylinders are not pointing toward the shear direction, were never observed in a steady shear flow in the bulk. Cylinders initially prepared orthogonal to shear rotated toward the shear direction.[22] These induced changes in block copolymer melts and solutions with hexagonal structures have been studied in great detail by many groups.[12] Usually, different techniques are combined to obtain useful information at different length scales because shear flow can affect both the texture and the interparticle correlations. The experimental techniques used to probe the structure under shear of such materials include optical microscopy, scattering of radiations, and NMR spectroscopy.[23]

The objective of this study was to investigate the influence of shear on the structure of the lyotropic hexagonal phases of an amphiphilic diblock copolymer. We used polystyrene-*b*-poly(acrylic acid, sodium salt), PS-PANa, aqueous solutions in the intermediate concentration regime. Different phase morphologies of PS-PANa have been obtained by varying the ratio of the hydrophobic polystyrene block length to the hydrophilic poly(acrylic acid) block length.[24,25] The samples chosen for this investigation had block lengths that favored out of equilibrium rodlike micellar morphologies.[26] The locked-in cylindrical morphology was specifically achieved by the fine-tuning of the copolymer micellar brush conformation through the control of the pH, thus leading to ionization of the polyelectrolyte poly(acrylic acid) block. We investigated the structure at rest of the copolymer aqueous solutions to get insight into the micelle shape and size, in the most diluted regime, and into their structural organization. Furthermore, we studied the swelling behavior of the micellar solutions as a function of polymer concentration by monitoring the shift of the main peak position in the scattering intensity measured by small-angle X-ray and neutron scattering techniques (SAXS and SANS, respectively). These structural investigations showed that the swelling of the micellar solutions was restricted to concentrated samples. The results were clear evidence for the existence of physical association between neighboring diblock copolymer cylinders. As a consequence, the organization of such connected cylinders under steady shear flow displayed an unusual orientation, with the long axis of the cylinders being oriented parallel to the gradient direction. The data are discussed in the context of the swelling behavior and interpreted as evidence for the existence of association between the cylinders such as entanglement of the micellar brushes or chemical links that may result from postpolymerization side reactions in view of the chemical structure of the diblock copolymer chains.

Materials and Methods

The polystyrene-*b*-poly(ethyl acrylate), PS-PEA, precursor diblock copolymer was synthesized by controlled radical polymerization in aqueous emulsion by the Rhodia Synthesis and Development Laboratory located in Cranbury, NJ. The sequential synthesis process involved the polymerization of styrene followed by the polymerization of ethyl acrylate by using *S*-(1-methoxycarbonyl)ethyl-*O*-ethyl xanthate as the reversible chain transfer agent for this two-step polymerization. This synthesis method was identified as macromolecular design via the interchange of xanthates (MADIX).[27]

The precursor chain had the following chemical structure:

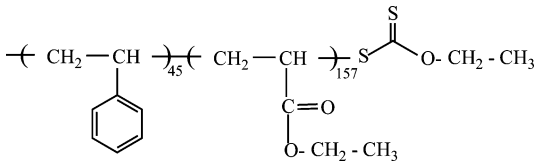

where the xanthate transfer agent group was localized at the chain end. The number average molecular weight and polydispersity of the PS first block, which was isolated prior to the addition of ethyl acrylate, and of the entire PS-PEA copolymer were determined by gel permeation chromatography (GPC, Phenogel columns calibrated by using standard PS) in tetrahydrofuran (THF) at 1 mL/min. The number average molecular weight and polydispersity were found to be 4700 g/mol and 2.3, respectively, for the styrene block, corresponding to 45 styrene monomers, and 15 700 g/mol and 2.2, respectively, for the ethyl acrylate blocks, corresponding to 157 ethyl acrylate monomers. This led to a PS weight fraction of 0.23. This value was further confirmed by NMR spectroscopy (Oxford AS400 MHz), performed on deuterated pyridine copolymer solution, which returned a PS weight fraction of 0.25. NMR data were obtained from the integration of peaks of the PS aromatic ring protons and the PEA methylene protons (chemical shifts located around 7.2 and 4.2 ppm, respectively).[28]

Subsequent to the synthesis and chemical characterization, the copolymer was hydrolyzed to yield the hydrophobic-hydrophilic diblock copolymer polystyrene-*b*-poly(acrylic acid, sodium salt), PS-PANa. This postpolymerization reaction consisted of adding dropwise, during 1 h, a 2 M aqueous solution of NaOH to an aqueous solution of PS-PEA at a concentration of 50 g/L at a temperature

(18) Zhang, Y.; Wiesner, U. *J. Chem. Phys.* **1995**, *103*, 4784−4793.
(19) Mortensen, K. *J. Phys.: Condens. Matter* **1996**, *8*, A103−A124.
(20) Schmidt, G.; Richtering, W.; Lindner, P.; Alexandridis, P. *Macromolecules* **1998**, *31*, 2293−2298.
(21) Tepe, T.; Schulz, M. F.; Zhao, J.; Tirrell, M.; Bates, F. S.; Mortensen, K.; Almdal, K. *Macromolecules* **1995**, *28*, 3008−3011.
(22) Scott, D. B.; Waddon, A. J.; Lin, Y. G.; Karasz, F. E.; Winter, H. H. *Macromolecules* **1992**, *25*, 4175−4181.
(23) Schmidt, G.; Muller, S.; Lindner, P.; Schmidt, C.; Richtering, W. *J. Phys. Chem. B* **1998**, *102*, 507−513.
(24) Bendejacq, D.; Ponsinet, V.; Joanicot, M.; Loo, Y.-L.; Register, R. A. *Macromolecules* **2002**, *35*, 6645−6649.
(25) Bhatia, S. R.; Mourchid, A. *Langmuir* **2002**, *18*, 6469−6472.
(26) Bendejacq, D.; Joanicot, M.; Ponsinet, V. *Eur. Phys. J. E* **2005**, *17*, 83−92.
(27) Destarac, M.; Charmot, D.; Franck, X.; Zard, S. Z. *Macromol. Rapid Commun.* **2000**, *21*, 1035−1039. Charmot, D.; Corpart, P.; Adam, H.; Zard, S. Z.; Biadatti, T.; Bouhadir, G. *Macromol. Symp.* **2000**, *150*, 23−32. Destarac, M.; Bzducha, W.; Taton, D.; Gauthier-Gillaizeau, I.; Zard, S. Z. *Macromol. Rapid Commun.* **2002**, *23*, 1049−1054. Chapon, P.; Mignaud, C.; Lizarraga, G.; Destarac, M. *Macromol. Rapid Commun.* **2003**, *24*, 87−91. Jacquin, M.; Muller, P.; Bauer, C.; Lizaragua, G.; Cottet, H.; Theodoly, O. *Macromolecules* **2007**, *40*, 2672−2682. Jacquin, M.; Muller, P.; Cottet, H.; Crooks, R.; Theodoly, O. *Langmuir* **2007**, *23*, 9939−9948.
(28) Grandjean, J. Ph.D. Thesis, Université Pierre et Marie Curie, 2003.

of 90 °C and under vigorous stirring. The reaction was continued for an additional 23 h at 90 °C. The resulting copolymer product, PS-PANa, was precipitated in an excess HCl solution to convert the PANa block to the pure, neutral poly(acrylic acid) block, PAA. Subsequently, the precipitated PS-PAA copolymer was isolated and dispersed in a mixture of H_2O and THF solution. We dialyzed this copolymer solution in regenerated cellulose membranes with a molecular weight cutoff of 6000−8000 (SpectraPor) against a reservoir of HCl aqueous solution at pH 2.5 for one week, and against deionized H_2O for another week. The solution in the reservoir was changed several times a day until the conductivity of the reservoir was stable and equal to that of a deionized H_2O reference solution. This purified precipitated copolymer in H_2O was finally freeze-dried and stored in a desiccator under reduced pressure prior to use. The efficiency of the hydrolysis reaction was controlled by proton NMR spectroscopy for the PS-PAA copolymer dissolved in deuterated pyridine. The extent of hydrolysis was found to be 0.98 ± 0.03, in agreement with previously reported results on hydrolysis of PS-PEA copolymers by NaOH.[29] We also titrated this copolymer with NaOH solution to check the molecular weight of the hydrolyzed PAA block. The final product, PS-PAA diblock copolymer, had a number average molecular weight of 4700−11 300 g/mol, while the neutralized product, PS-PANa diblock copolymer, had a molecular weight of 4700−14 760 g/mol.

The freeze-dried copolymer in its acidic form, PS-PAA, was dissolved in THF to a concentration of 150 g/L. This solution was poured in poly(tetrafluoroethylene) (PTFE) molds and left to dry under room conditions for 3−4 days to cast copolymer films with slightly less than 0.5 mm thickness. The films were additionally dried at room temperature under vacuum for 24 h and then at 60 °C for 1 h to completely remove the organic solvent, and they were finally reduced to a fine powder.

The powdered copolymer PS-PAA was directly dispersed to the desired concentration in sodium hydroxide H_2O solutions for rheology and SAXS studies or in sodium hydroxide D_2O solutions for SANS investigations. The fixed amounts of NaOH were chosen to precisely even out the number of acrylic acid monomers for each concentration so that the poly(acrylic acid) block was entirely converted to poly-(acrylic acid, sodium salt). The samples were then stirred and left to rest for at least 1 week prior to any measurement.

Rheology measurements were performed with a strain controlled rheometer (ARES Rheometrics) by using a cone and plate shear geometry at a constant temperature of 20 °C. The elastic and viscous moduli were measured as a function of frequency between 0.001 and 100 rad/s at a fixed applied strain chosen in the linear regime. The flow behavior of the samples was studied by recording the variation of stress with time as a function of the applied shear rate. Data were obtained in the form of steady shear stress as a function of the shear rate chosen between 0.01 and 1000 s^{-1}.

The copolymer in H_2O for concentrations in the range $30 \leq C \leq 100$ wt % was studied by small-angle X-ray scattering in transmission at the Laboratory for Research on the Structure of Matter, University of Pennsylvania, Philadelphia, PA. The setup consisted of a high brightness rotating anode that generated 1.54 Å X-radiations which scattered the samples contained either in cylindrical quartz cells or in rectangular cells sealed with mylar windows and held at room temperature. The scattered intensity was recorded by a multiwire area detector positioned at two different distances from the sample to yield wavevectors q between 0.005 and 0.1 $Å^{-1}$.

The suspensions in D_2O were studied by small-angle neutron scattering at the NIST Center for Neutron Research, located in Gaithersburg, MD, on the NG3 beamline for concentrations in the range $0.8 \leq C \leq 50$ wt %. The incident beam wavelength was 6 Å, and the area detector was positioned at two distances from the sample, 13.1 and 1.33 m, to cover scattering vectors q between 0.0035 and 0.3 $Å^{-1}$. The spectra were collected at room temperature for samples in quartz cells with a path length of 1 or 2 mm, depending on the concentration. D_2O was used to quantify the solvent scattering, and this was subtracted from the data. The spectra, which were also corrected for incoherent scattering estimated from the signal at high q, were subsequently obtained in absolute scale, [cm^{-1}]. Samples for SANS under shear were studied at CEA Laboratoire Léon Brillouin, LLB, located in Saclay, France, on the PAXY beamline at separated periods. The incident wavelength, selected between 6 and 14 Å, and the two sample-to-2D-detector distances, chosen between 1 and 2 m (short distance) and between 4 and 6 m (long distance), permitted us to cover scattering vectors q between 0.005 and 0.2 $Å^{-1}$. We used two shear cells transparent to neutrons to investigate the structure changes under shear at room temperature. The first shear cell was a couette type cell and consisted of an inner cylindrical stator of 22.5 mm radius and an outer cylindrical rotor of 23.5 mm radius. The samples were loaded in the shear cell and allowed to rest for a duration of 2 h. Data were collected for both radial and tangential configurations, with the neutron beam scattering the sample on the center and then on the edge of the couette cell, respectively, for each shear rate, starting from zero and going up to the highest value desired. The radial and tangential configurations corresponded to wavevectors along the velocity gradient and the velocity directions, and thus, the probed planes were the velocity−vorticity and velocity gradient−vorticity planes, respectively. The second shear cell was equivalent to a plate/plate geometry. It consisted of a thin hollow ring that holds the sample. The second part of the cell was a second rotating ring that closes the geometry. The characteristic dimensions of the cell (gap = 1 mm, width of the two rings = 3.5 mm) and its horizontal orientation with respect to the neutron beam, which crossed the lateral faces between the immobile and rotating rings, corresponded to the neutron beam along the vorticity axis and thus to the observation of the velocity−gradient plane. Details on this shear cell are given elsewhere.[30] We studied samples in the shear cells at rest (immobile cells) and at reliable shear rates between 1 and 50 s^{-1} with the couette cell and between 0.1 and 50 s^{-1} with the plate/plate cell. The scattering data collected at LLB were corrected for background and incoherent signals and obtained in absolute scale.

Results and Discussion

The birefringence of cast films was investigated by using a polarized-light microscope. The study confirmed the existence of strong birefringence in agreement with previous studies performed on these diblock copolymers with comparable molecular weights. These previous studies showed that the method of preparation described above yields long rodlike micelles where the PS block formed the core of the micelles and the PAA block was the shell structure.[26,28]

Upon neutralization of the PAA block by addition of NaOH and upon dilution, the copolymer aqueous solutions appeared slightly turbid. Samples at concentrations $C \geq 1$ wt % formed one macroscopic phase and were stable over a long period of time (more than 2 years). More diluted samples underwent phase separation that occurred within a few hours after preparation. The lower phase was slightly viscous and turbid, while the upper phase was a colorless nonviscous solution. Investigation of the turbid samples by cross-polarized optical microscopy confirmed the existence of typical liquid crystal textures reminiscent of strong birefringent polydomains.[23]

The upper curve in Figure 1 shows typical SAXS intensity for a PS-PAA powdered sample in the melt state, $C = 100$ wt %. The results are presented in the form I as a function of q which does not highlight structural features in the scattering intensity I. The data were integrated over the azimuthal angle, because the 2D scattering pattern was isotropic. Such a scattering picture

(29) Bhatia, S. R.; Crichton, M.; Mourchid, A.; Prud'homme, R. K.;Lal, J. *Polym. Prepr*. **2001**, *42*, 326−327. We performed a thorough study on partially hydrolyzed PEA blocks; however, we did not find noticeable changes in the data as a function of residual EA monomer fraction between 0 and 0.36. The results were shown in reference 28.

(30) Noirez, L.; Lapp, A. *Phys. Rev. Lett.* **1997**, *78*, 70−73.

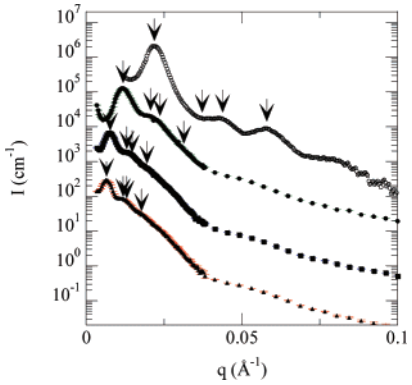

Figure 1. SAXS (upper curve) and SANS (lower curves) data on samples at $C = 100$, 20, 5, and 2 wt %, respectively, with error bars on SANS data. Downward arrows point to q values in the ratio of $1:\sqrt{3}:\sqrt{4}:\sqrt{7}$ characteristic of hexagonal order. The curves were vertically shifted for clarity.

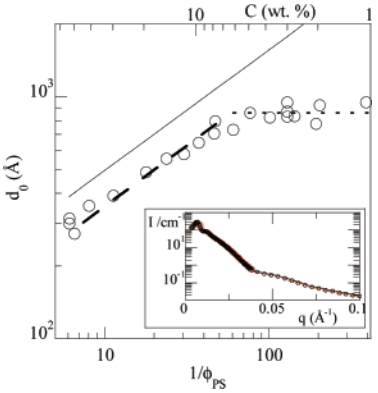

Figure 2. Correlation distance as a function of PS volume fraction (lower axis) and the corresponding concentration in wt % (upper axis). Solid line: theoretical power law for swelling of solutions of hexagonal-packed cylinders of 95 Å radius. Dashed oblique: least-square fit of the swelling law for $8 \leq C \leq 50$ wt %. Horizontal dashed line: asymptotic value for correlation distance (860 Å). Inset: SANS data on a sample at 2 wt % with error bars. Solid line: fit to the form factor for polydisperse cylinders with a mean radius of 95 Å and a polydispersity of 20%.

is typical of polydomain structures. Neutralized copolymer samples in D_2O were studied by SANS. Samples with $C < 1$ wt % that underwent a phase separation were centrifuged, and both the upper and lower phases were separately investigated by SANS. The corresponding data for representative PS-PANa copolymer samples at $C = 20$, 5, and 2 wt % are shown in Figure 1. We observed that the swollen PS-PANa copolymer solutions, similar to the melt PS-PAA copolymer, showed well-ordered polydomain structures, with successive correlation peaks located at q values in the ratio of $1:\sqrt{3}:\sqrt{4}:\sqrt{7}$ and shown by downward-pointing arrows in Figure 1, although the second and third peaks appeared as a large single bump probably due to a non-negligible copolymer polydispersity index. This sequence of peak positions was observed in the one-phase samples and in the lower phase for samples at $C < 1$ wt %. The scattering intensity of the upper phase of the two-phase solutions was very weak and suggested that the upper colorless nonviscous phase was water. The observed sequence of peak position confirmed that the samples were ordered arrays of hexagonal-packed cylinders. The second peak in the SAXS pattern, at a ratio $\sqrt{3}$ of the first peak, was weak because it was positioned very close to the first minimum of the form factor of cylinders for the melt copolymer.[31] It is worth adding that the scattering data were in agreement with cross-polarized light microscopy results which showed liquid crystal textures, and thus confirmed that the macroscopic samples were not uniformly aligned and that a polydomain structure was present.[20]

The similarities between the SAXS and SANS scattering curves at varying amounts of added water strongly suggested that the morphology of the micelles was cylindrical and was not altered upon neutralization of the poly(acrylic acid) block. The data also suggested that long-range structural order was preserved. These results were in agreement with previous studies which showed that PS-PAA block copolymers formed frozen-in micellar morphologies whose shape and size were affected neither by ionization of the PAA block by NaOH nor by dilution in water as long as the samples were not annealed at a temperature above the PS glass transition temperature, T_g.[26] The T_g of PS is far above the room temperature at which these samples were prepared and studied.[32]

Even though the scattering intensity of the most diluted samples studied was strongly impacted by the structure factor, which meant that the interactions between the micelles were not negligible, it was possible to get insight into the form factor of the micelles and more precisely into the PS micellar core characteristics. This is because, on the one hand, at sufficiently high values of momentum transfer q, the scattering intensity follows the variations of the form factor, since the structure factor reduces to unity and the scattering intensity approaches the product of the contrast factor by the form factor in this q range.[33] On the other hand, the contribution of the PANa block of this copolymer to the scattering intensity is always small because the contrast between this block and D_2O is weak compared to the PS to D_2O contrast.[34] Therefore, we chose to utilize the infinitely long polydisperse cylinder form factor to model scattering intensity in the q domain above the peak positions, $P(q,R_c)$. The polydisperse form factor accounts for the average PS core radius, R_c, of the cylinders and its distribution assuming a lognormal size distribution. It is given by the product of convolution of the distribution of radii and the form factor of infinitely long rigid cylinders given by $P(q,R_c) \sim [2J_1(qR_c)/qR_c]^2/q$, where J_1 is the first order Bessel function.[35,36] The data for a representative sample ($C = 2$ wt %) is shown in the inset of Figure 2 in the form of $I(q)$ versus q. It is worth adding that the so-called Porod presentation[36] highlights even more the contribution of the form factor to $I(q)$. The used bare-core model along with the approximation of infinitely long cylinders was shown to provide a good model for the form factor of these PS-PANa rodlike micelles.[37] Furthermore, the approximation of long rigid cylinders has been validated by atomic force microscopy and transmission electron microscopy observations of the PS-PANa micelles which demonstrated that the length of the cylinders was in the micrometer length scale at the least.[26] The polydisperse model matched well the oscillations of the form factor in the scattered intensity. The resulting fit validated the approximation we have used which neglected the contribution of the PANa corona to $I(q)$. The result in the inset of Figure 2 led to an estimate for the PS core radius, R_c, of 95 Å and a polydispersity of 20%.

The position of the first peak, q_0, is associated with the correlation length, $d_0 = 2\pi/q_0$, which represents the distance

(31) Honeker, C. C.; Thomas, E. L.; Albalak, R. J.; Hajduk, D. A.; Gruner, S. M.; Capel, M. C. *Macromolecules* **2000**, *33*, 9395−9406.
(32) Santangelo, P. G.; Roland, C. M. *Macromolecules* **1998**, *31*, 4581−4585.
(33) Groenewegen, W.; Egelhaaf, S. U.; Lapp, A.; van der Maarel, J. R. C. *Macromolecules* **2000**, *33*, 3283−3293.
(34) Grandjean, J.; Mourchid, A. *Phys. Rev. E* **2005**, *72*, 041503.
(35) Hamley, I. W.; Castelletto, V. *Prog. Polym. Sci.* **2004**, *29*, 909−948.
(36) Higgins, J. S.; Benoît, H. C. *Polymers and Neutron Scattering*; Clarendon Press: Oxford, 1994.
(37) Svaneborg, C.; Pedersen, J. S. *Macromolecules* **2002**, *35*, 1028−1037.

between adjacent (10) planes for a structure of HPC or the most densely packed layers of cylinders. The distance between the first neighboring cylinders can be calculated as $d_{c-c} = 2d_0/\sqrt{3}$. The results of SANS intensity shown in Figure 1 confirmed that the peak position q_0 shifts to low q values as the concentration decreases down to $C = 8$ wt %. However, a careful inspection of the SANS data suggested that q_0 did not show a noticeable shift when the concentration was between 1 and 8 wt %. To verify this inclination, we plotted the correlation length, d_0, as a function of the PS block volume fraction, ϕ_{PS}, for all the one-phase samples investigated. The choice of ϕ_{PS} as the varying parameter in solutions of core−shell copolymer morphologies was justified, since the core size was independent of concentration.[38] The PS volume fraction was calculated from the copolymer concentration and the molar volume of each constituent: D_2O, polystyrene, and poly(acrylic acid, sodium salt) which was 33.8 g/mol.[39] The copolymer swelling relation, which gives the evolution of the distance d_{c-c} with ϕ_{PS} is $d_{c-c}/d_c = (\phi/\phi_c)^{-1/D}$.[40] This relation is satisfied for homogeneous solutions of swelling cylinders. In this relation, d_c is the distance between cylinders at close packing, ϕ_c is the volume fraction at close packing, and D corresponds to the number of directions for the swelling. $D = 2$ and corresponds to the two radial directions of swelling. d_c is the diameter of the cylinders, and ϕ_c equals $\pi/2\sqrt{3}$ for an HPC structure. Thus, the swelling relation reduces exactly to $d_0 = (\pi\sqrt{3}/2)^{1/2} R_c \phi_{PS}^{-1/2}$.

The data of the swelling behavior are presented in Figure 2. The variation of the correlation length with $\phi_{PS} > 0.016$, which corresponded to $C > 6.5$ wt %, was remarkably described by a power law with an accurate exponent for the swelling of hexagonal-packed cylinders, although the theoretical equation overestimated the correlation length by nearly 40%. More significantly, a sharp departure from the swelling power law was depicted in the experimental data for copolymer concentrations $C < 6.5$ wt %. In this concentration regime, the swelling of the structure reached a saturation plateau and the correlation length leveled off to 860 Å with the addition of more water, which corresponded to an upper limit of 1000 Å for the cylinder−cylinder distance. Since the PS micellar core was frozen, the swelling of the samples by water for $C > 6.5$ wt % was directly linked to the swelling of the polyelectrolyte brushes of PANa. Below the limit of swelling of 6.5 wt %, the data suggested that addition of more water did not promote further cylinder−cylinder separation because the brushes were connected and held the micellar cylinders physically associated. It was thus likely that a microscopic phase separation took place. Pockets of water should have been present in the interstices between microdomains of the hexagonal phase. This hypothesis has been verified by optical microscopy which showed that, indeed, the samples were not homogeneous at the microscopic scale when $C < 6.5$ wt %.[28]

The effect of shear on these associated HPC solutions was investigated by SANS for samples at concentrations C between 3 and 6.3 wt %. It is worth noting that these samples formed strong viscoelastic solids, with an elastic modulus, G', at least 1 order of magnitude higher than the viscous modulus, G'', in the entire frequency range investigated by rheometry. Both G' and G'' did not vary significantly in this frequency range. Flow characterization of the micellar solutions showed that two instabilities appeared in their rheogram (shear stress versus shear rate curve) as presented in Figure 3. The samples were shear

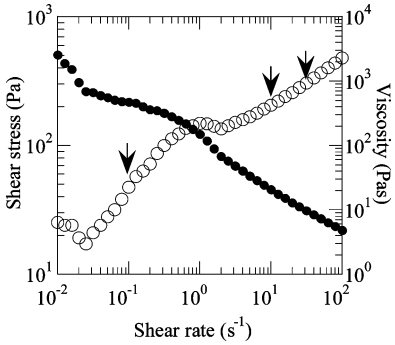

Figure 3. Evolution of steady shear stress (○) and viscosity (●) versus shear rate at $C = 5$ wt %. Downward arrows indicate the investigated shear rates in the plate/plate neutron cell.

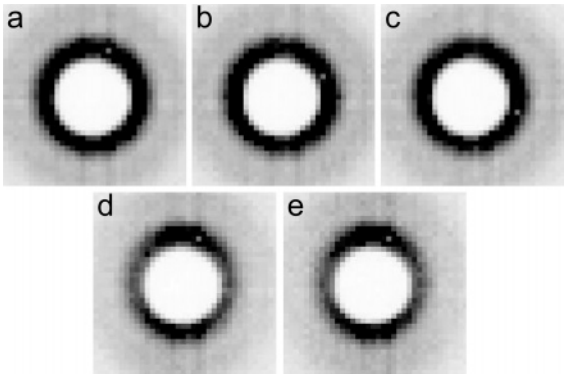

Figure 4. SANS patterns on a sample at $C = 6.3$ wt % in the couette cell. (a−c) Radial configuration at shear rates of 0, 1, and 50 s^{-1}, respectively, and (d and e) tangential configuration at shear rates of 1 and 50 s^{-1}, respectively. The observation planes are velocity−vorticity plane (a−c) and gradient−vorticity plane (d and e) (horizontal and vertical directions, respectively). Beamline configuration: wavelength = 6 Å and sample−detector distance = 6.790 m.

thinning, and the instabilities were located at very low and intermediate shear rates (∼0.05 and 1 s^{-1}, respectively). These instabilities are distinguishable in Figure 3 and correspond to secondary maxima of the stress curve and sharp decreases in the viscosity curve.

The presence of these instabilities raised the question of whether the association of the cylinders, as suggested from the swelling investigation, impacted the flow behavior of the solutions. For this purpose, SANS experiments under shear were carried out at shear rates chosen in the increasing parts of the shear stress curve above the observed instabilities. We studied micellar solutions in the concentration range between 3 and 8 wt % in the restricted swelling domain and immediately above the limit of swelling.

The resulting 2D SANS patterns are shown in Figure 4. These measurements were obtained on a sample at $C = 6.3$ wt % loaded in a couette, and the neutron beam was incident on the sample either in the center or at the edge of the couette cell and corresponded to radial and tangential configurations, respectively. The 2D SANS patterns, in the radial configuration, yielded a symmetric scattering ring for the three shear rates investigated: 0, 1, and 50 s^{-1} as presented in Figure 4a−c, respectively. We did not observe noticeable changes in the orientational or positional correlations between the cylinders as a consequence of shear rate. This observation was unusual for HPC solutions subjected to shear where the cylinders commonly orient parallel to the velocity direction.[15,19,20,23] Such common orientation would have yielded a strong Bragg peak along the vorticity direction

(38) Castelletto, V.; Fisher, J.; Hamley, I. W.; Yang, Z. *Colloids Surf., A* **2002**, *211*, 9−18.
(39) Hiraoka, K.; Yokoyama, T. *J. Polym. Sci., Part B: Polym. Phys.* **1986**, *24*, 769−778.
(40) Hyde, S. T. *Colloids Surf., A* **1995**, *103*, 227−247.

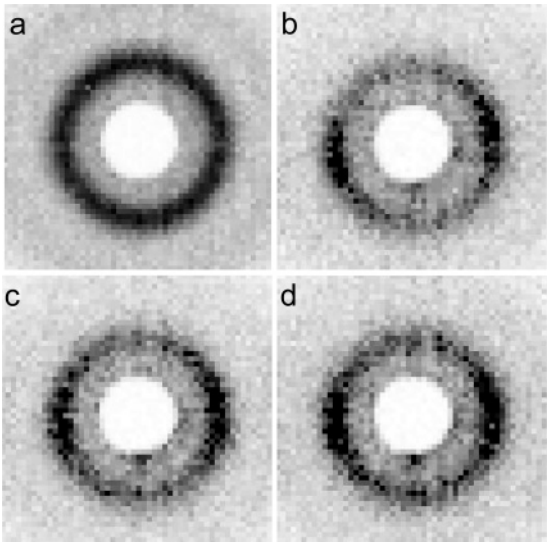

Figure 5. SANS patterns on a sample at $C = 5$ wt % in the plate/plate cell at shear rates of (a) 0, (b) 0.1, (c) 10, and (d) 30 s^{-1}. Observation plane: velocity (horizontal)−gradient (vertical). Beamline configuration: wavelength = 14 Å and sample−detector distance = 4.054 m.

(the vertical axis on the patterns). Further insight into the effect of shear on these HPC solutions was obtained through the tangential configuration studies that probed the vorticity−gradient plane. The resulting 2D scattering patterns were indeed highly affected by shear, and the scattering intensity was anisotropic as shown in Figure 4d and e for shear rates of 1 and 50 s^{-1}, respectively. Once more, the results are unusual for HPC solutions under shear for which one would have expected an isotropic correlation peak in this observation plane. Instead, the Bragg peak was preferentially highly intense in the neutral direction. These results strongly suggested that the rodlike micelles were aligned along the gradient direction. Similar SANS results were found with sheared samples investigated in the couette at $C =$ 3 and 5 wt %.

We extended the study of the structure under shear of these HPC solutions by using a plate/plate shear cell to probe the velocity−gradient plane. Figure 5 shows 2D scattering patterns at rest and at low and moderate shear rates (0, 0.1, 10, and 30 s^{-1}, shown in patterns a−d, respectively) for a sample at $C =$ 5 wt %. These measurements showed that the SANS pattern was isotropic at rest and became anisotropic under shear with the intense Bragg peak being observable in the velocity direction and signaling a preferential orientation along the gradient direction. The results were in agreement with the data of the SANS investigation of cylinders under shear in the couette cell. Moreover, the patterns of Figure 5 noticeably showed that the Bragg peaks of the sheared samples made a finite angle, of about 15°, with respect to the horizontal or velocity direction. This result is further enhanced in Figure 6, which displays the scattering intensity, I, at the peak position, q_0, as a function of the azimuthal angle, ψ, for shear rates of 0.1 and 30 s^{-1}. It suggested that the sheared cylinders were tilted with respect to the direction of flow. Similar SANS results were also found on sheared micellar solutions, prepared at $C = 3$ and 8 wt %, studied in the plate/plate shear cell.

Close inspection of the experimental data of the structure under shear reveals that the micellar cylinders in solution adopted the most unfavorable orientation, that is, along the gradient direction. These results contradict previous investigations of the structure under shear of anisotropic micellar copolymer solutions. However, in the light of the swelling behavior of the solutions, the shear

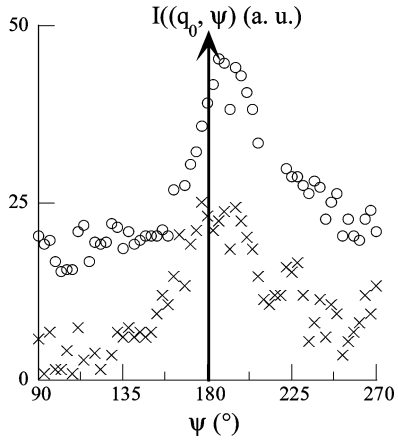

Figure 6. Variation of the SANS intensity at the correlation peak versus azimuthal angle at shear rates of (○) 0.1 and (×) 30 s^{-1} for the sample at $C = 5$ wt % investigated in the plate/plate cell. 180° corresponds to the horizontal axis or velocity direction. Data were vertically shifted for clarity.

induced orientation can be rationalized if one considers the consequence of physical links that connect the micellar brushes. Indeed, the study of the structure showed that the neighboring cylinders remained bound together as the system was diluted and the cylinders did not separate beyond 1000 Å. This observation suggests that the core−shell cylinders were physically associated, possibly owing to entanglement of the brushes or to chemical bonds between neighboring cylinders that might be formed during the preparation of the solutions. It is then reasonable to assume that they cannot be oriented as isolated cylinders in the flow field. We expect entanglement or chemical bonds between the hydrophilic brushes to prevent rotation of individual rodlike micelles along the neutral axis. Moreover, the condition of minimal drag resistance that confines the core of the block copolymer cylinders in the shear plane pointing toward the shear axis must be balanced by the constraint on the micellar brushes which tends to align them along the flow streamlines, at least at high shear rates, to minimize drag resistance on them. This second constraint favors a perpendicular orientation of the cylinder axis with respect to shear direction.

On the other hand, there should be a substantial shear resistance on aggregates formed by bounded cylinders as a whole. The resulting shear forces should significantly prevail over the drag resistance on the micellar core because they act on large sized aggregates, unless the shear forces are strong enough to break up the aggregated micellar cylinders. However, we did not notice any shift in the peak position for samples prepared on the plateau region of the swelling curve as a function of applied shear rate. Thus, we conclude that the applied shear rates do not break up the aggregates. Furthermore, the behavior of the solutions in the diluted regime strongly suggests that the energy of association between the micellar cylinders is high enough to promote phase separation. Since the aggregation of the micellar cylinders is due to the association of the brushes as deduced from the swelling investigation and the measured distance of separation of neighboring cylinders, the formed aggregates are envisioned to extend in the radial direction, in relation to the cylinder axis. Such networked micellar structures should consist of nearly 2D aggregated cylinders. Accordingly, these aggregates are expected to align akin to lamellar morphologies in the flow streamlines to minimize drag resistance. The resulting orientation is then assumed to resemble the parallel configuration for lamellae. Indeed, a schematic representation of one envisioned aggregate is shown in Figure 7, where we represent one layer of the cylinders

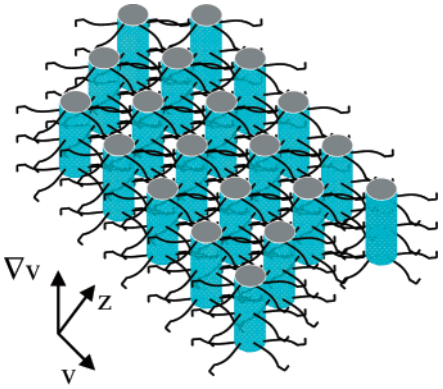

Figure 7. Schematic representation of the behavior of networked micellar cylinders subjected to shear and oriented parallel to gradient direction ∇v.

packed together in close contact to take into consideration the implication of the limited swelling result, and oriented parallel to the velocity gradient axis such as to fulfill the state of orientation deduced from the investigation of the structure under shear.

A comparable observation was reported for entangled lamellar diblock copolymers subjected to large amplitude dynamic strains where it was shown that the lamellae adopted the unexpected transverse orientation under shear.[18] The results were examined by presuming that the orientation of entangled brush chains along the shear direction overwhelms the penalty for the lamellar main core to stand the drag resistance by being perpendicular to this direction. Albeit the number average molecular weight of the polyelectrolyte brushes, that is, 14 760 g/mol, is not large enough to encourage chain entanglement, the synthesis method, which is characterized by a polydispersity index around 2, inherently leads to the existence of a rather high weight average molecular weight, that is, around 32 500 g/mol, for the PANa or 346 monomers. Entanglement of these significantly long copolymer chains should promote aggregation of neighboring cylinders. Indeed, our data show that the distance between two neighboring cylinders saturates to $d_{c-c} = 1000$ Å. This gives an average length of the brush $L_b = d_{c-c}/2 - R_c = 405$ Å and corresponds to the length of 152 acrylic acid monomers. Thus, the large copolymer chains belonging to neighboring cylinders inevitably overlap. Overlapping of long brush chains is a consequence of the full stretching of the polyelectrolyte block at the ionic strength where the samples were prepared, 0.0001 M, which is far below the critical concentration of Na counterions confined within the brushes. This critical concentration denotes the separation between the low ionic strength osmotic regime where the brushes are stretched and the salted regime where the brushes are compressed,[26,41] and it was estimated to be 0.38 M for this system.[28]

On the other hand, one should question the chemical characteristics of the copolymers synthesized by controlled radical polymerization. The reaction scheme involves dithiocarbamates as transfer agents, and these functional molecules are incorporated at the chain ends into the copolymer structure as shown in the chemical formula of the PS-PEA precursor copolymer. One feature of dithiocarbamates is their ability to hydrolyze using either amines or inorganic bases such as NaOH.[42] Under such alkaline conditions, the dithiocarbamate moiety is reduced to the corresponding thiol (−S−H) end group. The postpolymerization reaction that we employed to convert poly(ethyl acrylate) to poly(acrylic acid, sodium salt) uses a highly alkaline medium and high temperature, which should easily favor hydrolysis from dithiocarbamate to sulfhydryl end groups, thus leading to the following chain chemical structure:

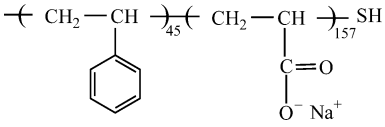

The formation of such sulfhydryl terminated copolymer chains does not influence the formation of core−shell micellar morphologies. In addition, we do not expect these functional end groups to induce attractive interactions between the micelles, such as H bondings. This is because S−H bonds are not appreciably polarized, due to the small difference in electronegativity between S and H. However, one important side reaction that might significantly affect the copolymer chain structure is a possible oxidation of the thiol end groups that would lead to the formation of disulfide bonds between two copolymer chains to give a PS-PANa-PS-like triblock copolymer whose structure is

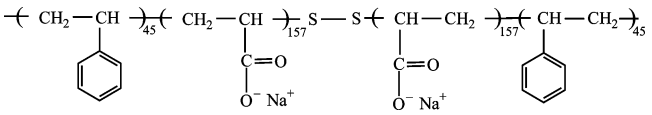

Thus, to what extent can the oxidation of the copolymer chains be facilitated under the conditions of synthesis, preparation, or storage of these diblock copolymers is an important issue to understand. This question requires one to examine the organosulfur chemistry, a key mechanism of the reaction of biomacromolecules. Autoxidation of thiols to disulfides under alkaline conditions was shown to take place with some thiol compounds.[43] The conditions of the reactions in this study, albeit in organic solvents, were quite similar to our own experimental conditions. It was demonstrated that disulfide bridges were feasible in alkaline solutions. A more recent study in the field has investigated the conditions of interconversion of thiols and disulfides under molecular hydrogen and oxygen atmospheres using organometal catalysts.[44] In probing the reactivity of many organothiol compounds, these authors have shown that the presence of a metal catalyst is a necessary condition to achieve the oxidation of thiol end groups with molecular oxygen. The major finding was that no oxidation took place in the absence of the organometal catalyst. This observation suggests that disulfide bridges are not likely between these PS-PANa diblock copolymers, more especially as the condition of manipulation and storage of the copolymer were carried out such as to avoid unnecessary exposure to air and no catalyst was present. Likewise, repetitive GPC analyses on the PS-PEA precursor copolymer did not return varying values of the molecular mass. This only indicates that significant end group oxidation did not occur: the molecular weight distributions of these copolymers are large enough that GPC is not sensitive to small formations of bridged triblock copolymers chains with molecular weights two times larger than that of the original diblock copolymer chains. It is worth adding that our extensive study of the structure and swelling behavior of PS-PANa spherical micelles synthesized by MADIX never showed restricted swelling behavior, in contrast to the present study of cylindrical micelles.[25,34,45]

(41) Pincus, P. *Macromolecules* **1991**, *24*, 2912−2919. Borisov, O. V.; Birshtein, T. M.; Zhulina, E. B. *J. Phys. II* **1991**, *1*, 521−526.
(42) Schilli, C.; Lanzendorfer, M. G.; Muller, A. H. E. *Macromolecules* **2002**, *35*, 6819−6827.
(43) Wallace, T. J.; Schriesheim, A.; Bartok, W. *J. Org. Chem.* **1963**, *28*, 1311−1314.
(44) Arisawa, M.; Sugata, C.; Yamaguchi, M. *Tetrahedron Lett.* **2005**, *46*, 6097−6099.
(45) Grandjean, J.; Mourchid, A. *Europhys. Lett.* **2004**, *65*, 712−718.

Conclusion

In the present study, we investigated the assembly of diblock copolymers in which the chemical parameters, as well as the method of preparation, yield out-of-equilibrium rodlike micelles, organized as hexagonal-packed cylinders in aqueous solutions. The data on the structures show that the micellar cylinders are formed from a frozen-in polystyrene core surrounded by polyelectrolyte poly(acrylic acid, sodium salt) brushes. The investigation of the SANS intensity of the diluted and concentrated solutions suggests that, in the high and intermediate concentration regimes, the swelling of the micelles follows the power law expected for hexagonal-packed cylinders. In the diluted concentration regime, the swelling analysis shows that the decrease in micellar concentration below a concentration threshold does not promote further separation between the micellar cylinders. These results are clear evidence for the existence of topological constraints between the copolymer micellar brushes. By monitoring the 2D SANS intensity of the micellar solutions under shear flow, we have shown that the cylinders orient parallel to the velocity gradient direction. This configuration is the most unfavorable orientation for hexagonal-packed cylinders. However, with regard to the swelling behavior of the micellar solutions, it is suggested that the observed structural orientation under shear is the consequence of these topological constraints that maintain the cylinders associated. A possible mechanism that may have been the origin of such association between the micellar cylinders is the oxidation of the thiol end groups and formation of bridges between the micelles. However, in the view of the conditions required to oxidize thiol compounds, it is likely that such side reaction does not occur to a large extent in this system. Entanglement of the large hydrophilic chains of this polydisperse copolymer could also be the cause of such behavior. Entanglement is likely because the data of the structure show that the large chains unambiguously overlap in the concentration regime studied. These data are in agreement with those of a previous investigation of entangled copolymer lamellae which showed that the shear promoted an unusual orientation instead of the commonly observed orientation of isolated objects under shear, but which were rationalized by considering the effect of topological constraints on the lamellae.

Acknowledgment. Support from the CNRS/Rhodia Inc. Complex Fluids Laboratory is gratefully acknowledged. We thank Dr. Gilda Lizzaraga of the Rhodia Synthesis and Development Laboratory for synthesizing and characterizing the PS-PEA copolymers. Sincere thanks are also due to Dr. Lizzaraga, Dr. Bzducha from Rhodia, Dr. Ghedeau-Boudeville from CNRS, and Dr. Jacquin from IFP for fruitful discussions on the chemistry of thiols. We acknowledge the support of the NIST, the U.S. Department of Commerce, and the CNRS/CEA joint Léon Brillouin laboratory in providing the neutron facilities used in this work. We especially thank Dr. Steve Kline and Dr. Boualem Hammouda for providing assistance at the NIST, Dr. Alain Lapp for assistance with the SANS measurements in the couette cell, and Dr. Laurence Noirez for assistance with the SANS measurements in the plate/plate cell. The SANS data are partially based upon activities supported by the National Science Foundation under Agreement No. DMR-9986442.

LA703764E